approximate magnitude of the distortion. These departures from axial symmetry are presumably due to lattice perturbations and suggest a broadly similar resistance to angular deformation for the two MCl_4^{2-} ions. The magnitude of the distortion ($\alpha - \beta \approx 20°$) in $(enH_2)_2ZnCl_6$ and its guest copper complex is quite striking. It is this that causes the marked rhombic component to the ligand field, thus producing the unusual ground state in $(enH_2)_2ZnCuCl_6$. The mixing coefficient of the d_{z^2} orbital in the angular-overlap calculations $b = 0.231$ is in good agreement with the value $b \approx 0.27$ from the simple analysis of the molecular g values (see previous section).

General Conclusions. The EPR and optical spectra of copper-doped $(enH_2)_2ZnCl_6$, Cs_2ZnCl_4, and Rb_2ZnCl_4 suggest that the guest $CuCl_4^{2-}$ ions in each case adopt a distorted-tetrahedral geometry. At 77 K the EPR spectrum of $(enH_2)_2Zn[Cu]Cl_6$ shows both hyperfine and superhyperfine structure. The chlorine superhyperfine tensors show a marked rhombic character, and the principal axes of these probably deviate significantly from the copper–chlorine bond directions. It is likely that this deviation is caused by the noncoincidence of the bond axes and the $d_{x^2-y^2}$ orbital lobe directions. It would therefore be of interest to study the anisotropy of the superhyperfine structure in other pseudotetrahedral chlorocuprate complexes. Angular-overlap calculations have been used to deduce the likely geometry of the $CuCl_4^{2-}$ guest ions, and in each case the distortions from a regular tetrahedral ligand arrangement can be interpreted in terms of an overall flattening caused by the asymmetry of the Cu^{2+} d-electron density, plus a rhombic component due to lattice perturbations. In $(enH_2)_2Zn[Cu]Cl_6$ the rhombic distortion is substantial, involving a difference of ~20° between the two ∠ClCuCl angles containing the molecular symmetry axis. As a consequence of this, the ground-state wave function of the complex consists of a mixture of the $d_{x^2-y^2}$ and d_{z^2} orbitals. Calculations of the kind described may prove of value in deducing the probable ligand coordination geometry of copper(II) ions in protein molecules.

Acknowledgment. The authors are indebted to the Central Science Laboratory of the University of Tasmania for providing facilities for the measurement of the EPR and low-temperature optical spectra and to J. Bignall for technical assistance. Financial assistance of the Australian Research Grants Commission (to M.A.H.) and the University of Tasmania (to R.J.D.) is gratefully acknowledged. The Humboldt Foundation and Professor D. Reinen of the Fachbereich Chemie of the University of Marburg are thanked by M.A.H. for providing financial assistance and laboratory facilities during the initial stages of the work.

Registry No. $(enH_2)_2ZnCl_6$, 70281-84-4; Cs_2ZnCl_4, 13820-35-4; Rb_2ZnCl_4, 33724-11-7; $CuCl_4^{2-}$, 15489-36-8; Cu, 7440-50-8.

Supplementary Material Available: A listing of the g^2 values measured for rotations of the magnetic field for different crystal planes of the compounds (3 pages). Ordering information is given on any current masthead page.

Contribution from the Departments of Chemistry, University of Denver, Denver, Colorado 80208, and University of Colorado at Denver, Denver, Colorado 80202

Metal–Nitroxyl Interactions. 36. Single-Crystal EPR Spectra of Two Copper Porphyrins Spin Labeled with Five-Membered Nitroxyl Rings

REDDY DAMODER, KUNDALIKA M. MORE, GARETH R. EATON,* and SANDRA S. EATON

Received August 16, 1983

Single-crystal EPR spectra have been obtained for two copper porphyrins spin labeled with five-membered nitroxyl rings. Multiple conformations were observed for each of the complexes doped into zinc tetraphenylporphyrin. The dependence of the electron–electron spin–spin splittings on the orientation of the crystal in the magnetic field was analyzed to obtain the isotropic exchange and anisotropic dipolar contributions to the interaction. The interspin distance, r, ranged from 9.3 to 13.5 Å. Values of the exchange coupling constant, J, ranged from -42×10^{-4} to $+35 \times 10^{-4}$ cm^{-1}. The range of values of J was greater than was previously observed for analogous complexes containing six-membered nitroxyl rings. The greater dependence of the value of J on the molecular conformation for the five-membered nitroxyl rings than for the six-membered nitroxyl rings may explain the previously observed large solvent and temperature dependence of the values of J for complexes containing five-membered nitroxyl rings.

Introduction

EPR studies of biological systems have demonstrated the importance of spin–spin interaction.[1] For some applications of the EPR interaction information it is desirable to separate the isotropic exchange and anisotropic dipolar contributions. The dipolar term is a measure of the distance between the two interacting spins. The exchange coupling constant is dependent on the bonding pathway between the two centers on which the electrons are localized. We have recently shown that the two contributions can be separated by the analysis of frozen-solution[2] and single-crystal EPR spectra.[3-5] Since the value of the exchange coupling constant J can be measured in fluid solution, it is important to determine whether that value of J can be used to estimate values in frozen solution or single crystals. The values of J observed for I–V in fluid solution

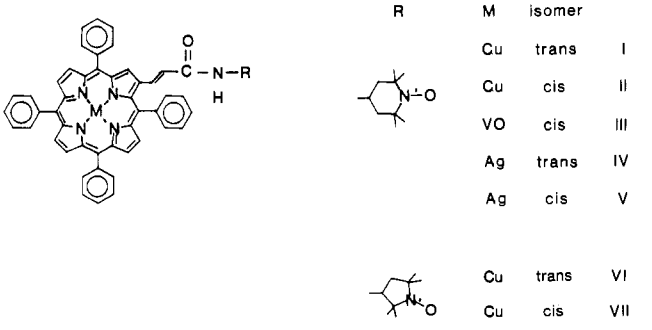

have been found to agree well with those observed in rigid media.[3-5] It can be anticipated that molecular flexibility can

* To whom correspondence should be addressed at the University of Denver.

(1) Blankenship, R. E. *Acc. Chem. Res.* **1981**, *14*, 163–170. Klimov. V. V.; Krasnovskii, A. A. *Photosynthetica* **1981**, *15*, 592–609. Schulz, C. E.; Devaney, P. W.; Winkler, H.; Debrunner, P. G.; Doan, N.; Chiang, R.; Hager, L. P. *FEBS Lett.* **1979**, *103*, 102–105.

0020-1669/84/1323-1320$01.50/0

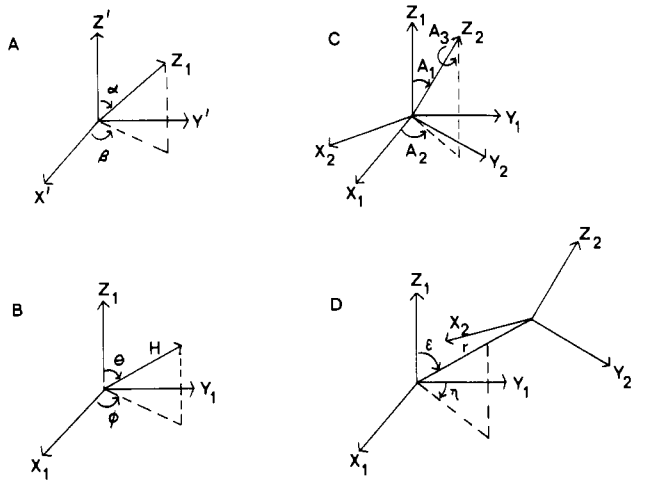

Figure 1. Definition of the orientation relationships: (A) angles α and β, defining the orientation of the copper z axis relative to the primed axes used for data collection; (B) angles θ and ϕ, defining the orientation of the magnetic field relative to the axes of the copper electron; (C) angles A_1 and A_2, defining the orientation of the nitroxyl axes relative to the copper axes; (D) angles ϵ and η, defining the orientation of the interspin vector r relative to the copper axes. Throughout the text r is used to denote the magnitude of the interspin vector.

result in conformational dependence on solvent, temperature, and steric effects. Thus both exchange and dipolar interactions are potentially environment dependent. To facilitate insightful applications of spin–spin interactions, it is necessary to obtain accurate interaction magnitudes for a wide range of complexes.

In fluid solution the values of J for complexes containing five-membered nitroxyl rings have generally been found to be greater than for analogous complexes containing six-membered nitroxyl rings.[6-9] The differences were greater when there was significant π character in the bonds connecting the metal and the nitroxyl ring[6-8] than when the spin–spin interaction was predominantly through σ orbitals.[9] However, for VI and VII, which contain five-membered nitroxyl rings, the values of J in fluid solution were substantially smaller than had been observed for the analogous complexes I and II, which contain six-membered nitroxyl rings.[10,11] The values of J for VI and VII were also strongly solvent dependent.

We have examined the oriented single-crystal EPR spectra of VI and VII doped into zinc tetraphenylporphyrin in order to compare the spin–spin interaction parameters with those previously obtained for VI and VII in fluid solution and for I and II in the same single-crystal host.

Experimental Section

Compounds VI and VII were prepared as reported in ref 10. The growth of the single crystals, mounting of the crystals, and data collection were performed as reported in ref 3–5. The angle between the z' axis used for data collection and the z axis of the copper **g** and **a** tensors (α in Figure 1A) was less than 2° for the crystal doped with VI and about 15° for the crystal doped with VII. The computer-simulated spectra of VII included a correction for the value of α.

Computer Simulations. The perturbation calculations used in the simulation of the spectra have been described previously.[2-5] The Hamiltonian (eq 1) consists of terms for independent electrons 1

$$\mathcal{H} = \mathcal{H}_1 + \mathcal{H}_2 + \mathcal{H}_{\text{int}} \quad (1)$$

$$\mathcal{H}_i = \sum_{j=x_i,y_i,z_i} (\beta g_j S_{ij} H_j + A_j S_{ij} I_{ij}) \qquad i = 1, 2 \quad (2)$$

$$\mathcal{H}_{\text{int}} = -JS_1 \cdot S_2 + \mathcal{H}_{\text{dipolar}} \quad (3)$$

(copper) and 2 (nitroxyl) (eq 2) and an interaction term that includes isotropic exchange and dipolar contributions (eq 3). The symbols in eq 1–3 have their usual meanings and are discussed in detail in ref 2 and 12. The splitting between the singlet and triplet levels is J, and a negative value of J indicates antiferromagnetic interaction. The angles that define the relative orientations of the axes of electrons 1 and 2, the dipolar tensor, and the magnetic field directions are shown in Figure 1.

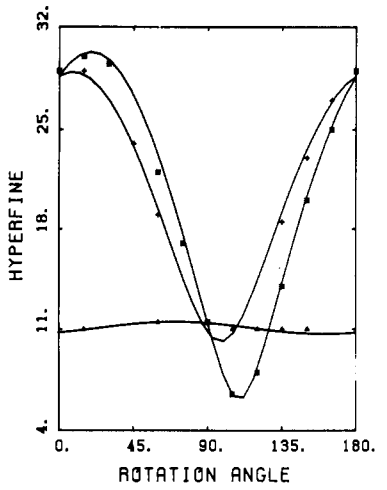

Figure 2. Plots of the orientation dependence of the nitroxyl nitrogen hyperfine splitting in gauss in three orthogonal planes for species 5 of trans isomer VI doped into ZnTPP. The experimental data are denoted as follows: (▲) $x'y'$ plane; (*) $x'z'$ plane; (+) $y'z'$ plane. The solid lines are the calculated curves.

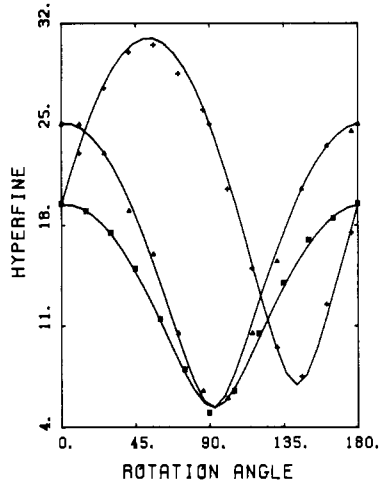

Figure 3. Plots of the orientation dependence of the nitroxyl nitrogen hyperfine splitting in gauss in three orthogonal planes for species 2 of cis isomer VII doped into ZnTPP. The experimental data are denoted as follows: (▲) $x'y'$ plane; (*) $x'z'$ plane; (+) $y'z'$ plane. The solid lines are the calculated curves.

(2) Eaton, S. S.; More, K. M.; Sawant, B. M.; Boymel, P. M.; Eaton, G. R. *J. Magn. Reson.* **1983**, *52*, 435–449.
(3) Damoder, R.; More, K. M.; Eaton, G. R.; Eaton, S. S. *J. Am. Chem. Soc.* **1983**, *105*, 2147–2154.
(4) Damoder, R.; More, K. M.; Eaton, G. R.; Eaton, S. S. *Inorg. Chem.* **1983**, *22*, 2836–2841.
(5) Damoder, R.; More, K. M.; Eaton, G. R.; Eaton, S. S. *Inorg. Chem.* **1983**, *22*, 3738–3744.
(6) Boymel, P. M.; Eaton, G. R.; Eaton, S. S. *Inorg. Chem.* **1980**, *19*, 727–735.
(7) Boymel, P. M.; Braden, G. A.; Eaton, G. R.; Eaton, S. S. *Inorg. Chem.* **1980**, *19*, 735–739.
(8) Sawant, B. M.; Shroyer, A. L. W.; Eaton, G. R.; Eaton, S. S. *Inorg. Chem.* **1982**, *21*, 1093–1101.
(9) Sawant, B. M.; Braden, G. A.; Smith, R. E.; Eaton, G. R.; Eaton, S. S. *Inorg. Chem.* **1981**, *20*, 3349–3354.
(10) More, K. M.; Eaton, G. R.; Eaton, S. S. *Inorg. Chem.* **1981**, *20*, 2641–2647.
(11) More, K. M.; Eaton, G. R.; Eaton, S. S. *Can. J. Chem.* **1982**, *60*, 1392–1401.
(12) Boas, J. F.; Hicks, P. R.; Pilbrow, J. R.; Smith, T. D. *J. Chem. Soc., Faraday Trans. 2* **1978**, *74*, 417–431.

Table I. g and A Values for the Copper[a,b] and Nitroxyl Electrons

electron	compd	species	g_{xx}	g_{yy}	g_{zz}	A_{xx}[c]	A_{yy}[c]	A_{zz}[c]
copper	VI	1-3, 5	2.049	2.049	2.202	24	24	198
copper	VI	4	2.049	2.049	2.201	24	24	201
copper	VII	1-4	2.05	2.05	2.201	24	24	198
nitroxyl	VI	1	2.0089	2.0066	2.0035	9	10	29
nitroxyl	VI	2	2.0085	2.0066	2.0028	5	10	29
nitroxyl	VI	3	2.0092	2.0071	2.0034	6	8	29
nitroxyl	VI	4	2.0085	2.0058	2.0035	8	9	26
nitroxyl	VI	5	2.0087	2.0066	2.0033	5	10	29
nitroxyl	VII	1	2.0085	2.0064	2.0028	6.5	6.5	28
nitroxyl	VII	2	2.0092	2.0069	2.0030	6.5	5	29
nitroxyl	VII	3	2.0083	2.0060	2.0022	7	7	30
nitroxyl	VII	4	2.0085	2.0066	2.0025	7	7	31

[a] The principal values of the porphyrin nitrogen hyperfine coupling tensor were $A_{xx} = 14.6 \times 10^{-4}$, $A_{yy} = 14.6 \times 10^{-4}$, and $A_{zz} = 17.4 \times 10^{-4}$ cm^{-1}. [b] A values are for ^{63}Cu. Both ^{65}Cu were included in the simulations. [c] In units of 10^{-4} cm^{-1}.

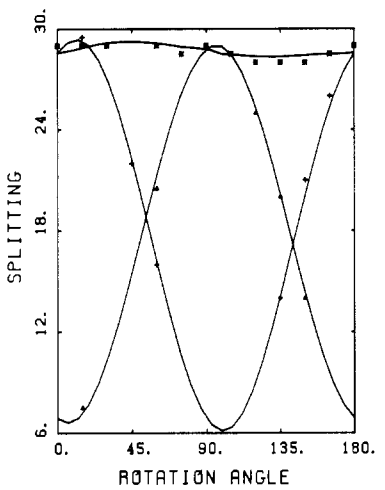

Figure 4. Plots of the orientation dependence of the spin–spin splitting in gauss in three orthogonal planes for species 5 of trans isomer VI doped into ZnTPP. The experimental data are denoted as follows: (▲) $x'y'$ plane; (*) $x'z'$ plane; (+) $y'z'$ plane. The solid lines are the calculated curves.

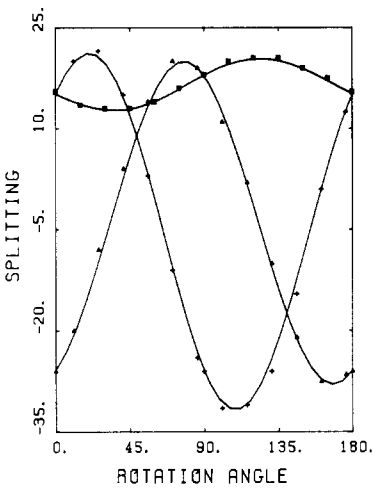

Figure 5. Plots of the orientation dependence of the spin–spin splitting in gauss in three orthogonal planes for species 2 of cis isomer VII doped into ZnTPP. The experimental data are denoted as follows: (▲) $x'y'$ plane; (*) $x'z'$ plane; (+) $y'z'$ plane. The solid lines are the calculated curves.

The orientation dependence of the nitroxyl hyperfine splitting and of the electron–electron spin–spin splitting was analyzed with the program ROTAN.[3] The adjustable parameters in the simulation of the orientation dependence of the spin–spin splitting are the isotropic exchange coupling constant J, the interspin distance r, and the orientation of the interspin vector, which is defined by the angles ϵ and η. Examples of the agreement between the experimental and calculated data are given in Figures 2–5. Since the copper **g** and **a** tensors were approximately axially symmetric, there was no molecular basis for a definition of the x and y axes. Therefore the values of η and A_2 are relative to the arbitrary axes used in the data collection. The values of the parameters obtained from ROTAN were then used to simulate the experimental spectra with use of the program CRYST.[3]

Analysis of EPR Spectra. Electron–electron spin–spin interaction between two $S = {}^1/_2$ centers results in a splitting of each hyperfine component of both electrons into AB doublets.[3-5] Since there was less nuclear splitting of the nitroxyl lines than of the copper lines, it was easier to obtain initial estimates of the spin–spin interaction from the nitroxyl lines than from the copper lines. Simulation of the complete spectra indicated that the values obtained from the nitroxyl lines were in good agreement with the spectra of the copper lines.

For both of the complexes, the assignments of nitroxyl lines to AB patterns was performed as previously reported for I–V.[3-5] In the crystal of ZnTPP doped with trans isomer VI, five distinguishable species were characterized. For cis isomer VII four species were observed. At some orientations of the crystal additional weak lines were observed, which were not assigned. It is likely that these lines are due to additional species with lower populations or broader lines, but the lines for these species were not resolved at enough orientations to adequately define them. There were more unassigned lines in the spectra of trans isomer VI than in the spectra of cis isomer VII. Overlap of the assigned lines with unassigned lines led to a greater uncertainty in the parameters for VI than for VII. A broad underlying signal was observed in all of the spectra. Similar signals have been seen in the crystals doped with I–V, and possible explanations have been discussed.[5]

The signals from the five species present in the crystal doped with trans isomer VI were distinguished as follows. Species 1 and 2 had the broadest lines and the largest values of J. The lines from these two species were resolved from the rest of the lines when the sum of the nitrogen hyperfine splitting and the spin–spin splitting was large enough to cause the lowest and highest field nitroxyl lines to be separated from the nitroxyl lines of the other species. The contributions from species 1 and 2 could be distinguished from each other on the basis of the differences in the values of ϵ, η, and r. Species 3 was readily distinguished because the orientation of the nitroxyl z axis for this species was substantially different from those of the other species. Its lines were resolved at most orientations in the xy plane and at some orientations in the xz plane. Species 4 and 5 had higher populations than the other three species, which facilitated assignment of these lines. Contributions from 4 and 5 were distinguished on the basis of differences in the values of ϵ, η, and r. The lines for 4 and 5 were resolved at most orientations in the yz plane and some orientations in the xz plane.

The contributions from the four species in the crystal of cis isomer VII were distinguished as follows. Species 1 had the lowest population, and its contributions to the spectra were well resolved primarily near the z axis. Species 2 had the highest population and the sharpest lines and dominated the spectra at most orientations of the crystal. The contributions from species 3 and 4 were well resolved primarily near the z axis and appeared as pairs of lines separated by the difference in the values of J for the two species (13 G). The z axis of the nitroxyl **a** tensor was oriented substantially differently for these two species than for species 1 and 2. The lines for species 4 were sharper than the lines for species 3.

Table II. Orientation and Interaction Parameters[a]

complex	species	A_1	A_2	ϵ	η	r[b]	J[c]	$d_\parallel$[c,d]	population, %
VI	1	30	60	117	−50	11.5	−42	−27	14
VI	2	15	60	78	−10	13.5	−40	−17	14
VI	3	90	25	105	30	13.0	9	−19	14
VI	4	25	120	62	35	11.5	−24	−27	27
VI	5	20	70	100	84	13.5	−20	−17	31
VII	1	63	−1	145	35	9.3	7	−52	8
VII	2	68	−2	126	76	10.2	−2	−39	46
VII	3	23	−18	144	77	9.4	35	−50	23
VII	4	32	−27	146	82	9.3	22	−52	23

[a] Angles are defined in Figure 1 and are in degrees. [b] In angstroms. [c] In units of 10^{-4} cm^{-1}. [d] Dipolar splitting for the orientation at which the magnetic field is parallel to the interspin vector.

The g values and nuclear hyperfine coupling constants obtained from the simulations of the spectra are given in Table I. The parameters obtained for the copper electron are in good agreement with those obtained for I and II.[3] The parameters for the nitroxyl electron are similar to those obtained for the piperidinyl oxyl in I–V.[3-5]

The values of the angles defining the relative orientations of the tensors and the values of the spin–spin interaction parameters are given in Table II. The dipolar splittings calculated for the orientation of the crystal at which the magnetic field is parallel to the interspin vector ($d_\parallel$) are also included in Table II. The uncertainties in the parameters for trans isomer VI are as follows: angles, ±10°; r, ±1.0 Å; J, ±4 × 10^{-4} cm^{-1}. For cis isomer VII the uncertainties are as follows: angles, ±5°; r, ±0.5 Å; J, ±2 × 10^{-4} cm^{-1}.

Due to the extensive overlap of the lines in the spectra, it was difficult to determine line widths accurately for most of the species. The line widths for species 2 of cis isomer VII were less uncertain than for the other species because it dominated the spectra at many orientations. For this species, which has J close to zero, the line widths varied from 2.5 to 5.0 G. There was no apparent correlation between the line widths and the magnitude of the dipolar interaction. However, it is not known how much of the line width variation is due to the orientation dependence of the unresolved proton hyperfine splitting. The nitroxyl line widths for the other species of cis isomer VII were as follows: species 1, 3–6 G; species 3 and 4, 4–12 G. For trans isomer VI the nitroxyl line widths were as follows: species 1 and 2, 5–15 G; species 3–5, 2.5–7 G. The copper line widths were between 2.5 and 10 G and were dependent on the value of m_I. This dependence was not included in the computer simulations.

Results and Discussion

Figure 6 shows the EPR spectra of trans isomer VI doped into zinc tetraphenylporphyrin obtained for $\theta = 30°$ and $\phi = 90°$. The copper nuclear hyperfine splitting at this orientation was 173 G for species 4 and 170 G for the other species. The porphyrin nitrogen hyperfine splitting for all the species was 15 G. These values are consistent with an orientation 30° away from the copper z axis. Twelve nitroxyl lines were clearly resolved at this orientation. The zero crossing points for the lines calculated for each of the species are marked below the calculated spectrum. The nitroxyl nitrogen hyperfine splittings for species 1 and 2 were 31 and 30 G, respectively, and the spin–spin splittings were 59 and 41 G, respectively. The highest field lines for these species were easily identified, the center four lines for each were obscured by the sharper nitroxyl lines from the other species, and the lowest field lines were broad and were partially superimposed on the copper lines. For species 3 the nitrogen hyperfine splitting was 8 G and the spin–spin splitting was 2 G, so its spectrum appeared to be a simple three-line pattern. The nitrogen hyperfine splitting for species 4 was 28 G, and the spin–spin splitting was 17 G. Five of the six lines for species 4 were well resolved. The nitrogen hyperfine splitting and spin–spin splitting for species 5 were both about 30 G, so its spectrum was an apparent four-line pattern, which was clearly resolved.

Figure 7 shows the EPR spectra of trans isomer VI obtained at $\theta = 90°$ and $\phi = 45°$. The copper hyperfine splitting was 25 G, and the porphyrin nitrogen hyperfine splitting was 16.5 G. The zero crossing points calculated for the nitroxyl lines for each of the species are marked below the simulated spectrum. The nitroxyl nitrogen hyperfine splittings for species

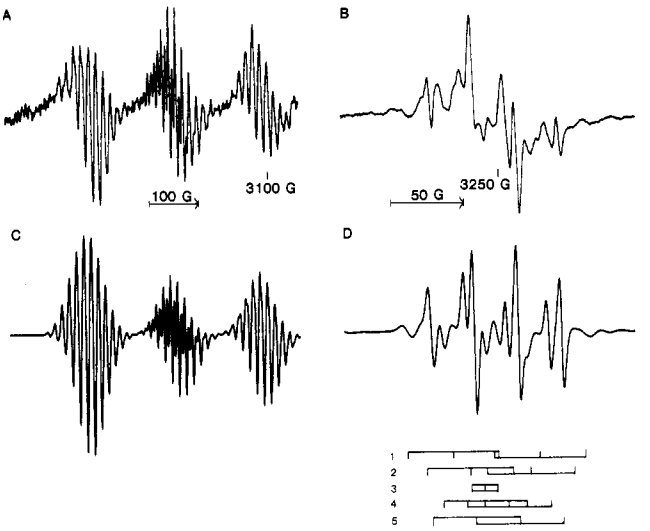

Figure 6. X-Band (9.105-GHz) EPR spectra of trans isomer VI doped into ZnTPP obtained at $\theta = 30°$ and $\phi = 90°$: (A) 600-G scan of the copper lines; (B) 200-G scan of the high-field portion of the spectrum; (C, D) corresponding calculated spectra. The spectra in A and B were obtained with 2-G modulation amplitude and 5-mW microwave power. The gain for A was 4 times that for B.

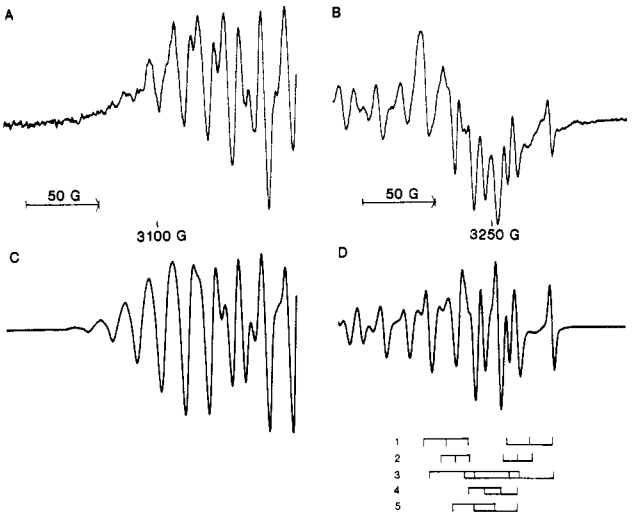

Figure 7. X-Band (9.106-GHz) EPR spectra of trans isomer VI doped into ZnTPP obtained at $\theta = 90°$ and $\phi = 45°$: (A) 200-G scan of the copper lines; (B) 200-G scan of the high-field portion of the spectrum; (C, D) corresponding calculated spectra. The spectra in A and B were obtained with 2-G modulation amplitude and 5-mW microwave power. The gain for A was 3.2 times that for B. There is a 50-G overlap of the spectra in A and B.

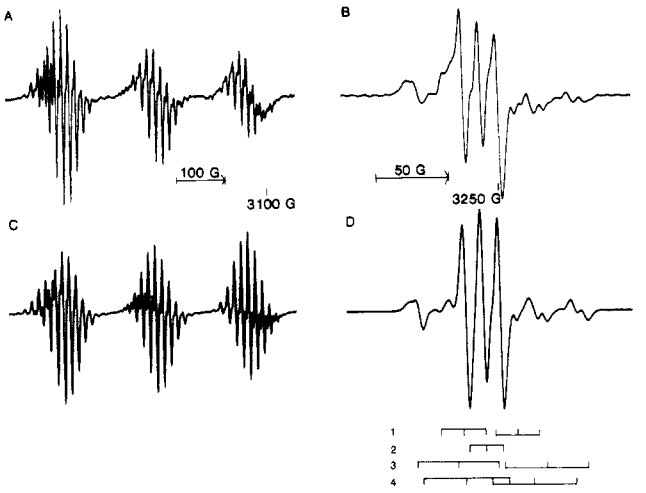

Figure 8. X-Band (9.107-GHz) EPR spectra of cis isomer VII doped into ZnTPP obtained at $\theta = 0°$: (A) 600-G scan of the copper lines obtained with 2-G modulation amplitude and 5-mW microwave power; (B) 200-G scan of the high-field portion of the spectrum obtained with 1.25-G modulation amplitude and 5-mW microwave power; (C, D) corresponding calculated spectra. The overall amplification for A is 4 times that for B.

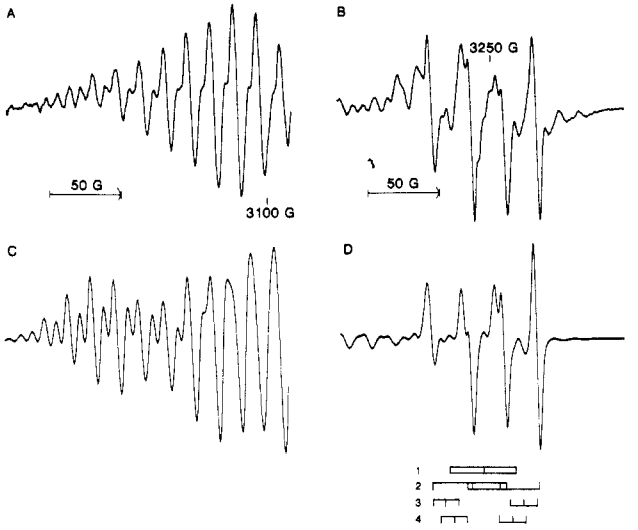

Figure 9. X-Band (9.107-GHz) EPR spectra of cis isomer VII doped into ZnTPP obtained at $\theta = 105°$ and $\phi = 16°$: (A) 200-G scan of the copper lines obtained with 2-G modulation amplitude and 5-mW microwave power; (B) 200-G scan of the high-field portion of the spectrum obtained with 1.25-G modulation amplitude and 5-mW microwave power; (C, D) corresponding calculated spectra. The overall amplification for A is 10 times that for B. There is a 10-G overlap of the spectra in A and B.

1 and 2 were 16 and 10 G, respectively, and the spin–spin splittings were 57 and 42 G, respectively. The lines for these species were not well resolved at this orientation. The nitrogen hyperfine splitting for species 3 was 30 G, and the spin–spin splitting was 24 G. The six lines for this species were well resolved. The nitrogen hyperfine splitting and spin–spin splitting for species 4 were both about 11 G, so its spectrum was an apparent four-line pattern, which was partially resolved. The nitrogen hyperfine splitting and spin–spin splitting for species 5 were both about 15 G. The apparent four-line pattern for this species was partially resolved. Part of the copper spectrum is shown along with the spectrum of the nitroxyl lines in Figure 7B. The relative intensities of the two portions of the spectrum are in reasonable agreement. Such agreement could not be achieved if some of the species that gave unresolved lines at this orientation were omitted from the simulation. Both portions of the spectrum are distorted by the broad underlying signal that was mentioned above.

Figure 8 shows the EPR spectra of cis isomer VII obtained at $\theta = 0°$. At this orientation the magnetic field is along the copper z axis so the hyperfine splitting was equal to A_{zz} and the g value was equal to g_{zz}. The zero crossing points calculated for the nitroxyl lines in the four species are indicated below the simulated spectrum. The nitrogen hyperfine for species 1 was 16 G, and the spin–spin splitting was 37 G. Its lines were poorly resolved at this orientation. The nitrogen hyperfine splitting for species 2 was 10 G, and the spin–spin splitting was less than the line width, so it gave rise to the apparent three-line pattern that dominated the spectrum. The nitrogen hyperfine splittings for species 3 and 4 were 29 and 30 G, respectively, and the spin–spin splittings were 62 and 48 G, respectively. The lines for this species that did not overlap with the triplet from species 2 were well resolved. The large difference between the nuclear hyperfine splittings for species 1 and 2 and those for species 3 and 4 and the differences in the spin–spin splittings for the four species facilitated the analysis of this spectrum.

Figure 9 shows the EPR spectra of cis isomer VII obtained at $\theta = 105°$ and $\phi = 16°$. At this orientation the copper nuclear hyperfine was 56 G and the porphyrin nitrogen nuclear hyperfine was 16 G. The nitroxyl region of the spectrum was dominated by the lines of species 2, which had a nitrogen nuclear hyperfine splitting of 24 G and a spin–spin splitting of 28 G. Since the nitrogen hyperfine splitting was slightly smaller than the spin–spin splitting, the two triplets were partially overlapped to give an apparent four-line spectrum with partially resolved splitting of the two center lines. The simulated spectrum includes the contributions for all four species and is consistent with the interpretation that the other three species are present, although the lines were not well resolved.

When spin-labeled copper porphyrins VI and VII are doped into the single crystal of ZnTPP, the spin-labeled side chain could be located at any of the eight pyrrole carbons and could be located above or below the porphyrin plane. Thus there are 16 possible locations for the substituent. Locations that are related by rotation around the copper z axis (normal to the porphyrin plane) or by reflection in the porphyrin plane are distinguishable by EPR, but locations that are related by inversion are indistiguishable at all orientations of the crystal. Thus there are eight possible distinguishable locations. In addition different side-chain conformations are potentially distinguishable. In the crystal doped with VI, five locations of the side chain were observed. For VII two locations were observed. The locations were characterized by different values of η and in one case by values of ϵ less than and greater than 90° for the same value of η. Since the side chains at the different orientations gave rise to different values of ϵ and of the spin–spin interaction parameters, they must be due to different species and not simply to different orientations in the crystal of identical species. Some of the differences between the species may result from differences in steric effects of the host crystal on the conformation of the spin-labeled side chain. We have arbitrarily chosen to keep the value of η between ±90°. However, since the Hamiltonian is invariant to inversion, the orientation $\epsilon = 117°$ and $\eta = -50°$ is indistinguishable from $\epsilon = 63°$ and $\eta = 130°$.

The values of η observed for trans isomer VI were −50, −10, 30, 35, and 84°. The 40–50° increments between the values of η are consistent with the angular increments expected for locations at successive pyrrole carbons around the porphyrin periphery as sketched in VIII. For the two species with η about 30° one has ϵ greater than 90° and the other has ϵ less than 90°. Thus these two species have the side chain on opposite sides of the porphyrin plane or at the inversion-related locations.

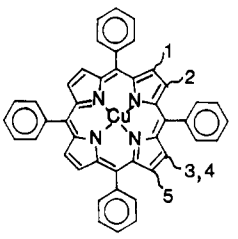

VIII

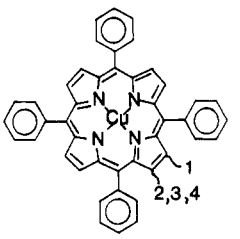

IX

For cis isomer VII the values of η were 35, 76, 77, and 82°. The locations of the side chains in these species are sketched in IX. Since the three species with η about 80° all have ϵ greater than 90°, they must be located on the same side of the porphyrin plane or at the inversion-related location. Species 3 and 4 have rather similar spin–spin interaction parameters, but species 2 is significantly different. It would appear that even small conformational differences caused by the steric effects of the host have a substantial impact on the spin–spin interactions. In sketches VIII and IX it is arbitrarily assumed that the x and y axes lie along the phenyl rings because there is no molecular basis for a definition of the x and y axes. None of the conclusions in this discussion are dependent on the orientations of these axes.

The values of r for trans isomer VI ranged from 11.5 to 13.5 Å. The values of ϵ ranged from 62 to 117°. In view of the inversion symmetry of the spectra the values of ϵ could also be viewed as ranging from 62 to 80° (Table II). The values of r for the cis isomer VII ranged from 9.3 to 10.2 Å, and in view of the inversion symmetry of the spectra the values of ϵ can be considered to range from 34 to 54°. The values of r for all the species are plotted as a function of ϵ in Figure 10. The data for complexes I, II, IV, and V are also included in Figure 10. The data for the vanadium complex III are not included because the points fall on a different curve. The difference has been attributed to the fact that the vanadyl ion is out of the plane of the porphyrin, which changes the relationship between the values of ϵ and r.[4] The points for complexes VI and VII systematically fall below the line that characterizes the six-membered nitroxyl rings. The deviation is in the direction of a shorter distance r at a given value of ϵ. Such a deviation is consistent with the smaller dimensions of the five-membered pyrrolidinyl ring in VI and VII than of the piperidinyl ring in I–V. The fact that the points for VI and VII fit the same general pattern as observed for the other complexes indicates that the overall geometries of the side chains are similar for the series of complexes.

The values of J for both VI and VII were found to vary significantly between species, indicating that the exchange interaction is sensitive to the detailed conformations of the bonds between the moieties on which the two unpaired electrons are located. However, the values in Table II indicate well-defined patterns. Except for one of the lower population species the values of J for trans isomer VI were large and negative. There was a range of values of J for cis isomer VII, but the average value was smaller than for trans isomer VI, and the values were positive or close to zero. These patterns are in good agreement with the results obtained for the analogous complexes I–V, which contain piperidinyl oxyl radicals.[3-5] The values of J observed for the four species of trans copper complex I were -30×10^{-4} to $+1 \times 10^{-4}$ cm^{-1}[3] while the range for trans complex VI was -42×10^{-4} to $+9 \times 10^{-4}$ cm^{-1}. Similarly the values of J for the four species of cis copper complex II were -4×10^{-4} to $+10 \times 10^{-4}$ cm^{-1}[3] and the range for cis complex VII was -2×10^{-4} to $+35 \times 10^{-4}$ cm^{-1}. Thus for both of the isomers the values of J for the six- and five-membered nitroxyl rings are of similar magnitude but there is a greater range of values for the five-membered nitroxyl rings (VI and VII) than for the six-membered nitroxyl rings (I and II). Since the acrylamide linkage used to attach the nitroxyl ring to the porphyrin was the same for I–VII, the differences may be due to the nitroxyl ring rather than the intervening linkage. The range of conformations accessible to the pyrrolidinyl ring may have a greater impact on the magnitude of the exchange interaction than do the range of conformations accessible to the piperidinyl ring. X-ray crystal structures of five-membered nitroxyl rings have shown that the pyrrolidinyl ring adopts a half-chair conformation with considerable variation in the bond angles.[13,14] In some cases there may be through-space interaction between the unpaired spin density on the amide proton and the pπ orbital on the nitroxyl nitrogen.

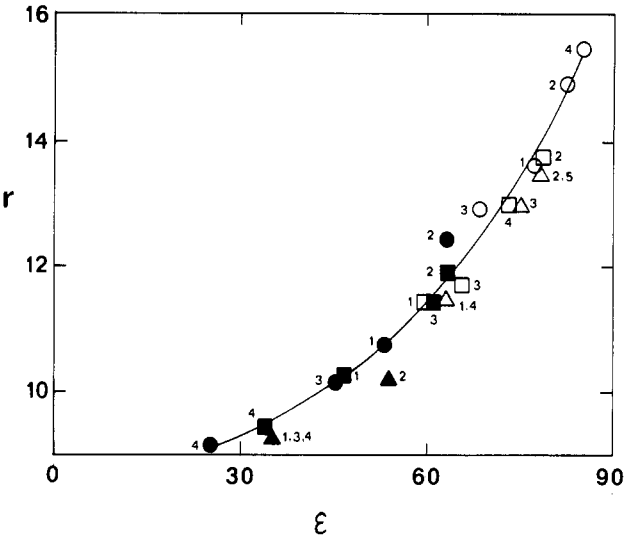

Figure 10. Plots of the values of r and ϵ for spin-labeled complexes I (○), II (●), IV (□), V (■), VI (△), and VII (▲). Each data point is labeled with the number of the species to which it corresponds. The solid line connects the data points for complexes I, II, IV, and V.

In fluid solution in a variety of solvents the values of J for trans isomer I were 18×10^{-4} to 25×10^{-4} cm^{-1} while the values for trans isomer VI were 3×10^{-4} to 5×10^{-4} cm^{-1}.[11] Comparisons with the values cited above for I and VI in the single-crystal host indicate that the agreement between the values of J in fluid solution and in the single crystal is much better for I than for VI. Apparently the single-crystal host preferentially stabilizes conformations of the five-membered nitroxyl ring, which are different than the preferred conformations in fluid solution. In fluid solution the value of J for cis isomer VII was much smaller in coordinating solvents ($<10 \times 10^{-4}$ cm^{-1}) than in noncoordinating solvents (up to 550×10^{-4} cm^{-1}).[10] Since the single crystal was grown in THF solution, the conformation of VII in the crystal would be expected to be similar to the ones observed in coordinating solvents in fluid solution. The small values of J for species 1 and 2 (Table II) are similar to the values observed in fluid solution, but the values for species 3 and 4 are substantially larger. Thus it appears that the use of values of J obtained for pyrrolidinyl spin-labeled complexes in fluid solution to estimate values in rigid media may be less reliable than for piperidinyl spin-labeled complexes.

Conclusions

Single-crystal EPR spectra of VI and VII doped into zinc tetraphenylporphyrin indicated the presence of five confor-

(13) Chion, B.; Lajzerowicz, J. *Cryst. Struct. Commun.* **1978**, *7*, 395–398. Chion, B.; Lajzerowicz, J.; Bordeaux, D.; Collet, A.; Jacques, J. *J. Phys. Chem.* **1978**, *82*, 2682–2688 and references therein.
(14) Guseinova, M. K.; Mamedov, S. D.; Amiraslanov, J. R.; Kutovaga, T. M. *Zh. Strukt. Khim.* **1978**, *19*, 97–101 and references therein.

mations of VI and four conformations of VII. The interspin distances were between 11.5 and 13.5 Å for VI and between 9.3 and 10.2 Å for VII. The electron-electron spin-spin coupling constant J was negative for most of the conformations of VI and positive for most of the conformations of VII. There was no correlation between the values of r and J. The range of conformations accessible to the five-membered nitroxyl rings appears to have a greater impact on the value of the exchange coupling constant J than the range of conformations accessible to the six-membered nitroxyl rings.

Acknowledgment. This work was supported in part by NIH Grant No. GM 21156.

Registry No. VI, 77629-59-5; VII, 77698-50-1.

Contribution from the Departments of Chemistry, University of Denver, Denver, Colorado 80208, and University of Colorado at Denver, Denver, Colorado 80202

Metal-Nitroxyl Interactions. 37. Single-Crystal EPR Spectra of a Spin-Labeled Copper Complex Containing an Imine-Urea Linkage

REDDY DAMODER, KUNDALIKA M. MORE, GARETH R. EATON,* and SANDRA S. EATON

Received August 16, 1983

Single-crystal EPR spectra have been obtained for a spin-labeled copper complex containing an imine-urea linkage. Six conformations of the molecule were observed in the zinc tetraphenylporphyrin host. The dependence of the electron-electron spin-spin splittings on the orientation of the crystal in the magnetic field was analyzed to obtain the isotropic exchange and anisotropic dipolar contributions to the interaction. The interspin distance, r, ranged from 10.0 to 14.0 Å. Values of the exchange coupling constant, J, ranged from -81×10^{-4} to $+37 \times 10^{-4}$ cm^{-1}. There was no correlation between the values of r and J. Comparison of the values of r and J for this complex with values obtained previously for spin-labeled copper complexes containing cis and trans acrylamide linkages indicated that isomers with cis and trans conformations of the imine linkage were present in the crystal.

Introduction

In a recent series of reports we have shown that detailed information concerning molecular geometry and electron-electron spin-spin coupling constants can be obtained from the analysis of frozen-solution and single-crystal EPR spectra of spin-labeled transition-metal complexes.[1-5] Substantial differences in the values of the electron-electron spin-spin coupling constants and interspin distances were observed for the cis and trans isomers of complexes I-IV, which have an

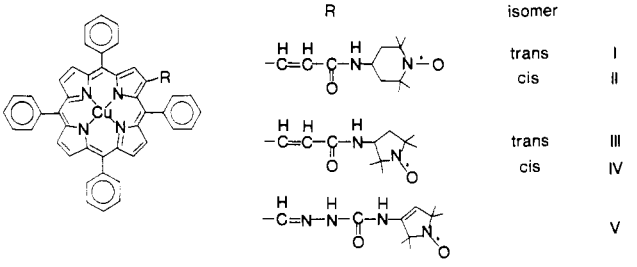

acrylamide linkage between a metalloporphyrin and a nitroxyl ring.[2,5] In fluid solution a single species was observed in the EPR spectra of V. The lines remained sharp at temperatures as low as -60 °C, which indicated that any dynamic processes occurring in solution that interconverted species with different values of the exchange coupling constant J must have activation energies less than about 8 kcal/mol.[6] The values of J were strongly solvent dependent. It was therefore of interest to determine the conformation of V that was present in solution. We have examined the single-crystal EPR spectra of V doped into a single crystal of zinc tetraphenylporphyrin in order to compare the spin-spin interaction parameters observed for the conformations in the crystal with the values of J observed in fluid solution.

Experimental Section

Compound V was prepared as reported in ref 6. The imine linkage in V is hydrolytically unstable, so the single crystal of zinc tetraphenylporphyrin doped with V was grown in a Kewaunee glovebox under a nitrogen atmosphere. Other aspects of the single-crystal preparation, mounting of the crystal, and data collection were performed as reported in ref 2-4. The angle between the z' axis used for data collection and the z axis of the copper **g** and **a** tensors (α in Figure 1A) was less than 3°, so it was assumed that $x = x'$, $y = y'$, and $z = z'$.

Analysis of EPR Spectra. The analysis of the single-crystal EPR spectra of spin-labeled metal complexes has been discussed previously.[2-5] The electron-electron spin-spin coupling splits each hyperfine component for both of the electrons into an AB doublet. Since there is less nuclear hyperfine splitting of the nitroxyl lines than of the copper lines, it is easier to identify the AB doublets for the nitroxyl lines than for the copper lines, so the initial estimates of the orientation and spin-spin interaction parameters were obtained from the nitroxyl lines. The orientation dependence of the spin-spin splitting of the nitroxyl lines was analyzed with the computer program ROTAN.[2] The adjustable parameters are the isotropic exchange coupling constant J, the interspin distance r, and the orientation of the interspin vector, which is defined by the angles ϵ and η. The values of the spin-spin interaction parameters were then used to simulate the complete experimental spectra. The simulations indicated that the parameters obtained from the nitroxyl lines were in good agreement with the spectra of the copper lines.

In the crystal of ZnTPP doped with V six distinguishable species were characterized. At some orientations of the crystal additional weak lines were observed, which were not assigned. It is likely that these lines are due to additional species with lower populations or

* To whom correspondence should be addressed at the University of Denver.

(1) Eaton, S. S.; More, K. M.; Sawant, B. M.; Boymel, P. M.; Eaton, G. R. *J. Magn. Reson.* **1983**, *52*, 435-449.
(2) Damoder, R.; More, K. M.; Eaton, G. R.; Eaton, S. S. *J. Am. Chem. Soc.* **1983**, *105*, 2147-2154.
(3) Damoder, R.; More, K. M.; Eaton, G. R.; Eaton, S. S. *Inorg. Chem.* **1983**, *22*, 2836-2841.
(4) Damoder, R.; More, K. M.; Eaton, G. R.; Eaton, S. S. *Inorg. Chem.* **1983**, *22*, 3738-3744.
(5) Damoder, R.; More, K. M.; Eaton, G. R.; Eaton, S. S. *Inorg. Chem.*, preceding paper in this issue.
(6) More, K. M.; Eaton, G. R.; Eaton, S. S. *Inorg. Chem.* **1983**, *22*, 934-939.

0020-1669/84/1323-1326$01.50/0